

DOI: <https://dx.doi.org/10.21123/bsj.2022.7178>

## Heavy Metal Complexes of 1, 2, 3-Triazole derivative: Synthesis, Characterization, and Cytotoxicity Appraisal Against Breast Cancer Cell Lines (MDA-MB-231)

Jihan Hameed Abdulameer <sup>1\*</sup> Mahasin F. Alias <sup>2</sup> <sup>1</sup>College of Education for Pure Sciences, University of Kerbala, Iraq.<sup>2</sup>Department of Chemistry, College of Science for Women, University of Baghdad, Iraq.\*Corresponding author: [Jihan.hameed@uokerbala.edu.iq](mailto:Jihan.hameed@uokerbala.edu.iq)E-mail addresses: [mahasinfa\\_chem@csu.uobaghdad.edu.iq](mailto:mahasinfa_chem@csu.uobaghdad.edu.iq)

Received 10/3/2022, Accepted 14/6/2022, Published Online First 25/11/2022

This work is licensed under a [Creative Commons Attribution 4.0 International License](https://creativecommons.org/licenses/by/4.0/).

### Abstract:

New chelating ligand derived from triazole and its complexes with metal ions Rhodium, Platinum and Gold were synthesized. Through a copper (I)-catalyzed click reaction, the ligand produced 1,3-dipolar cycloaddition between 2,6-bis((prop-2-yn-1-yloxy) methyl) pyridine and 1-azidododecane. All structures of these new compounds were rigorously characterized in the solid state using spectroscopic techniques like: <sup>1</sup>HNMR, <sup>13</sup>CNMR, Uv-Vis, FTIR, metal and elemental analyses, magnetic susceptibility and conductivity measurements at room temperature, it was found that the ligand acts as a penta and tetradentate chelate through N<sub>3</sub>O<sub>2</sub>, N<sub>2</sub>O<sub>2</sub>, and the geometry of the new complexes are identified as octahedral for (Rh & Pt) complexes and for (Au) complex square planner. The newly prepared compounds were designed and efficiently synthesized to be used to investigation of their toxicity bioassay (in vitro) as anticancer agent towards MDA cell lines. From the results obtained from cytotoxic assay, it can be concluded that the synthesized compounds are promising as new anticancer candidates in future especially in high concentration.

**Keywords:** Bioassay, Ligand chelates complexes, MDA cell line, Methoxy Group, Toxicity, Triazol.

### Introduction:

According to the World Health Organization's most current data, carcinoma is the world's second leading cause of death. More than 9.6 million deaths occur each year, accounting for roughly a quarter of all mortality. Several anticancer medications have been significantly improved in recent years. Nonetheless, the majority of currently available anti-cancer medications are ineffective, and side effects such as drug-induced impedance may arise. As a result, identifying and improving innovative, safe, and effective long-term cancer treatments with fewer side effects is crucial <sup>1</sup>. The 1,2,3-triazole and 1,2,4-triazole groups are two types of triazole are the basic units of many therapeutic medications, and their analogies have sparked the curiosity of medicinal chemists for a long time <sup>2</sup>. Triazole-containing heterocycles are lead molecule architectures that have attracted researchers' interest due to their broad range of biological effects, including anticancer <sup>3</sup>, characteristics that are antimicrobial, antitubercular, anti-HIV, anti-

convulsant, antibacterial, anti-inflammatory, analgesic, and antiviral <sup>2</sup>. Click chemistry reactions is important in medicinal chemistry and chemical biology cannot be overstated <sup>4</sup>. It is a potent and adaptable technology that can be used to design new anticancer drugs based on platinum and a better understanding of their biological actions at the level of the cell. To increase tumor targeting, new azide-alkyne cycloaddition techniques are being employed to functionalize Pt-based complexes with bio molecules <sup>5</sup>. Click-based detection, separation, and tracking of Platinum drug surrogates in biological and cellular settings also gives crucial information about Pt-based pharmacological modes of action and resistance <sup>6</sup>. Inorganic Pt-click reactions, however less well-studied, allow the production of novel (potentially multimetallic) Pt complexes as well as realistic methods for adding functional groups and monitoring Pt-azido drug localization <sup>7</sup>. The target of this study is to look into the anticancer properties of

Rhodium, Platinum, and Gold complexes that contained a chelating 1, 2, 3-triazole derivative.

## Materials and Methods:

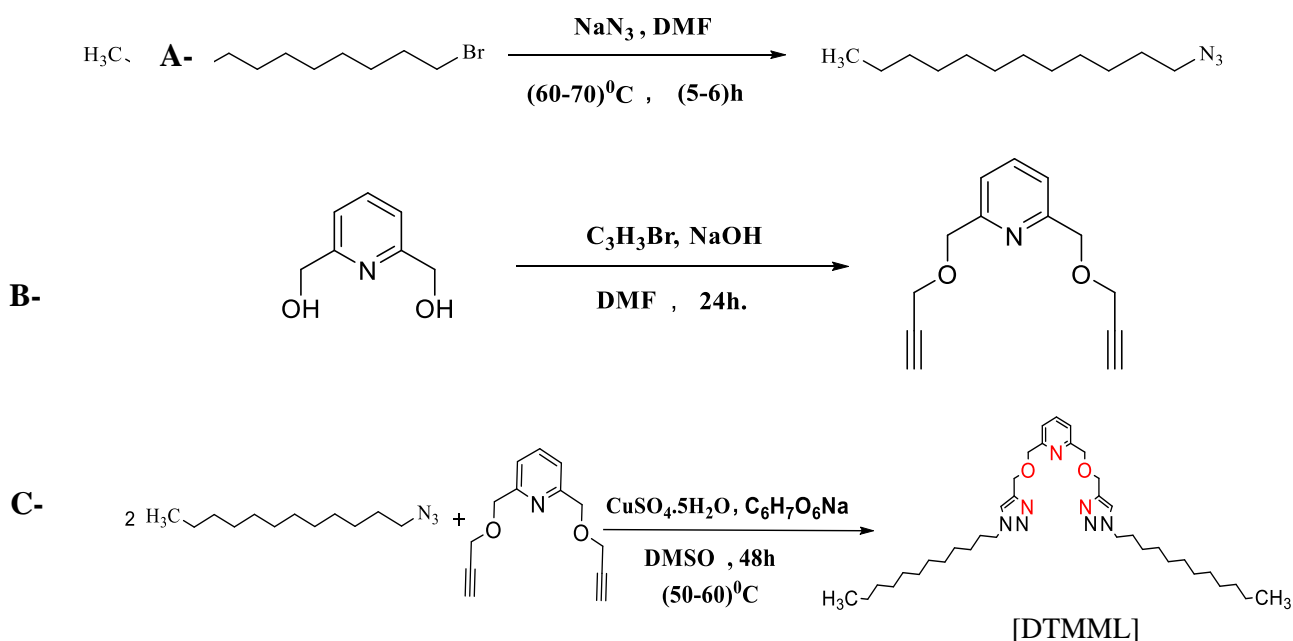
### Materials:

Whole of both the solvents and the chemicals used in the process of synthesis of new compounds were achieved from Sigma-Aldrich and Merck. The Agilent spectrometer (FT-IR 8400S SHIMADZU Spectrophotometer) was used to measure FTIR-spectra of prepared complexes and their ligand in the solid-state at the range of wavenumber at 4000-400 & 4000-200  $\text{cm}^{-1}$  using KBr & CsI pellets. The measurement of electronic spectra of all prepared compounds was obtained in liquid state by the instrument (UV-1800 PC) Shimadzu spectrophotometer at  $\lambda_{\text{range}} = 190\text{--}1100$  nm using quartz cell of 1 cm. Bruker DPX spectrometers operating at 600 MHz were used to obtain NMR spectra. Mass spectra were recorded on DIRECT

PROBE. The Euro EA3000 analyzer was used for the determined (C, H, and N) contents. Melting points were examined in open glass capillaries. The electrical conductivity meter (WTW), and magnetic susceptibility of complexes at 25°C were determined. Thin layer chromatography was employed to adjust the reaction and the silica plates were used (60 F254, 0.2 mm), which carried alkaline potassium permanganate dip.

### Synthesis of 2,6-bis(((1-dodecyl-1H-1,2,3-triazol-4-yl) methoxy) methyl) pyridine (DTMML)<sup>8,9</sup>

The preparation of the ligand was in accordance with the methods that described in the previous our work in literature<sup>9</sup>, where the methods consist of three steps (synthesis both of 1-azidododecane [AZD] and 2,6-bis((prop-2-yn-1-yloxy) methyl) pyridine [BPMPD]) which reacted with each other to prepare the employing ligand (DTMML) as shown as in scheme 1.



**Scheme 1. Shows the sequential steps to prepare the ligand [DTMML].**

### Metal-Complexation:

The current work includes using (1mmol) of the metal salts [ $\text{RhCl}_3$  (0.209g),  $\text{H}_2\text{PtCl}_6$  (0.486g), and  $\text{HAuCl}_4 \cdot \text{H}_2\text{O}$  (0.411g)] in an ethanoic solution undergoes the reaction and (0.637g, 1mmol) the ligand is added to an ethanoic solution of mineral salts while stirring (10 ml) in a (1:1) molar ratio. The mixture of reaction was refluxed for a few hours (2-3 hours) under heating<sup>10</sup>. Colorful precipitates were formed during this period, they were filtered several times and washed with ether then left to dry in a desiccator. As indicated in Table. 1, Spectroscopic, analytical and physical techniques were used to characterize all the complexes generated.

### Cytotoxic assay

The effect of cytotoxicity of complexes with their ligand were determined using the colometric 3-(4,5-dimethyl thiazole-2-yl)-2,5-biphenyl. The MDA-231 cell lines used in this work were obtained from Al-Nahrain University's biotechnology center. After 24 hours of treatment with the compounds at various doses, cell lines were examined. MTT assay results showed for all ligands and their heavy metal complexes using different doses (400,200,100,50,25,12.5 $\mu\text{g/ml}$ ) and compared with negative control culture medium without treatment<sup>11</sup>.

## Results and Discussion:

The resulting complexes and its chelated were colored powders that remained stable in the open atmosphere for a long period. Table 1 lists the

physio-chemical properties of resulting compounds. The results of the metal analysis agree with the calculated values in a satisfactory manner. Measurements of spectral and magnetic moments backed up the proposed molecular formula.

**Table 1. Summary of physical and analytical data for synthesized substances.**

Compound ds.	Color	Molecular weight g/mol	Melting point °C	Yield %	Elemental analysis Found (calc.)			Metal % found (calc.)	Suggested Molecular formula
					C%	H%	N%		
L	White	637.96	104-106	94.3	69.23 (69.66)	9.46 (9.95)	15.04 (15.37)	–	C <sub>37</sub> H <sub>63</sub> N <sub>7</sub> O <sub>2</sub>
L-Rh <sup>3+</sup>	Light brown	847.21	125-126	78	52.11 (52.40)	7.15 (7.43)	11.09 (11.57)	11.91 (12.15)	C <sub>37</sub> H <sub>63</sub> Cl <sub>3</sub> RhN <sub>7</sub> O <sub>2</sub>
L-Pt <sup>4+</sup>	Yellowish orange	974.84	133-135	80.1	45.13 (45.54)	6.21 (6.46)	9.87 (10.05)	19.96 (20.01)	C <sub>37</sub> H <sub>63</sub> Cl <sub>4</sub> PtN <sub>7</sub> O <sub>2</sub>
L-Au <sup>3+</sup>	Orang	941.27	162-163	89.4	47.09 (47.17)	6.32 (6.70)	10.18 (10.41)	20.43 (20.92)	C <sub>37</sub> H <sub>63</sub> Cl <sub>3</sub> AuN <sub>7</sub> O <sub>2</sub>

## Infrared spectroscopic study

A study of Infrared spectroscopy with CsI disc was used to record all of the spectra in the solid state. FT-IR provided useful information on the ligand [L] behavior with various heavy metal ions based on a comparison with published data<sup>12</sup>. The chemical 1-azidododecane was synthesized using the SN2 reaction in DMF dodecyl bromide with sodium azide. The extremely distinctive absorption of azide group at 2094 cm<sup>-1</sup> which is shown in the Fig. 1, is a strong evidence for the synthesis of the compound 1-azidododecane<sup>13</sup>. Fig.2 shows the spectrum of the compound [BPMP]. The reaction was successful, as demonstrated by the elimination of a broad band at (3354.79) cm<sup>-1</sup> and the emergence of sharp bands in the areas (3308.03 and 2121.77) cm<sup>-1</sup>. The terminal alkyne groups (C–H and C≡C) are responsible for these effects<sup>14</sup>. Fig.3 also provides a strong evidence that the cycloaddition reaction was successful, with bands disappearing around (2094 and 2117.91) cm<sup>-1</sup>, signaling the formation of the aromatic triazole ring, and weak bands appearing at (3093.29 and 1683.91) cm<sup>-1</sup> which indicated that the cycloaddition reaction was successful<sup>15</sup>.

The observed bands of free ligand L spectrum which are located in the regions (3093.29, 3138.29, 1595.18, 1505.04, 1220.98 and 1122.61) cm<sup>-1</sup> are attributed to the frequencies  $\nu(\text{C-H})_{\text{Pyridine}}$ ,  $\nu(\text{C-H})_{\text{Triazole}}$ ,  $\nu(\text{N=N})_{\text{Triazole}}$ ,  $\nu(\text{C=N})_{\text{Pyridine}}$ ,  $\nu(\text{C-N})_{\text{Triazole}}$ ,  $\nu(\text{C-O-C})_{\text{Ether}}$  respectively<sup>14,16</sup>.

The frequency of (N=N) shifted to a greater level around (2-85) cm<sup>-1</sup> in the complexes, and the frequencies of  $\nu(\text{C-N})_{\text{Triazole}}$ ,  $\nu(\text{C-O-C})_{\text{Ether}}$  and  $\nu(\text{C=N})_{\text{Pyridine}}$ , changed to a higher frequency in the vicinity of (14-54) cm<sup>-1</sup>, (28-31) cm<sup>-1</sup>, and (47-48) cm<sup>-1</sup>, respectively<sup>17</sup>. New bands for  $\nu(\text{M-N})_{\text{pyridine}}$ , appeared at (271.69, 273.34) cm<sup>-1</sup> in the complexes (Rh and Pt) respectively, as well as  $\nu(\text{M-O})$ , which appeared in the range (414-443) cm<sup>-1</sup>, and  $\nu(\text{M-N})_{\text{triazole}}$  that appeared at (516-588) cm<sup>-1</sup> in the complexes spectra. Other bands are shown in Table. 2, besides  $\nu(\text{M-Cl})$ , which appeared at (322.12, 308.62) cm<sup>-1</sup> in the complexes of Rh and Pt respectively<sup>18</sup>. As a result of these findings, the proposed in the range of complexes exhibit four and six coordination as a square planer and octahedral structure in solid state Figs. (4-6).

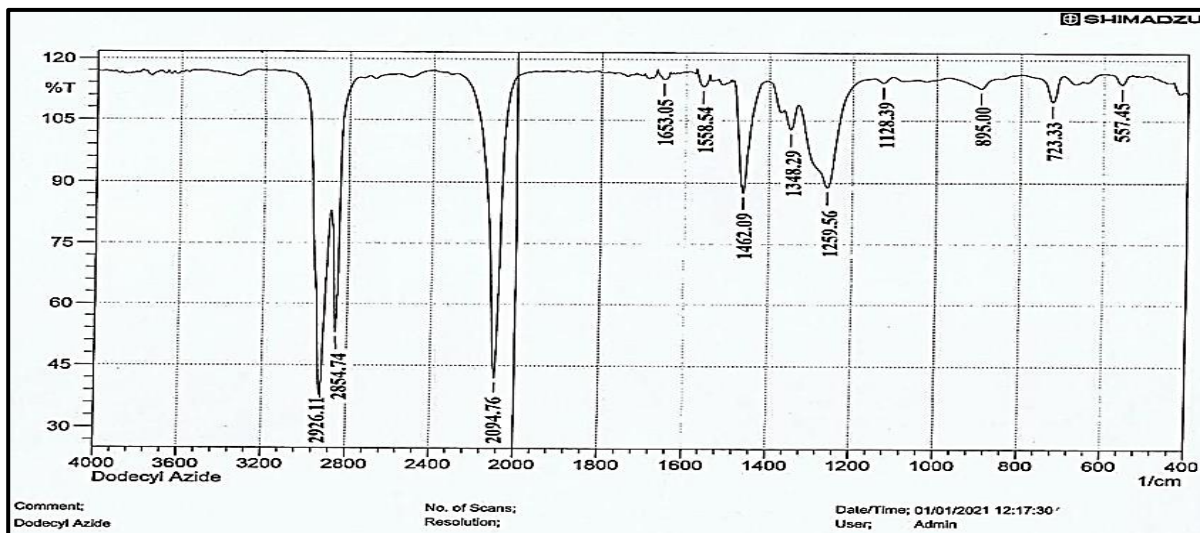


Figure 1. The spectrum of FT-IR of [AZD] compound.

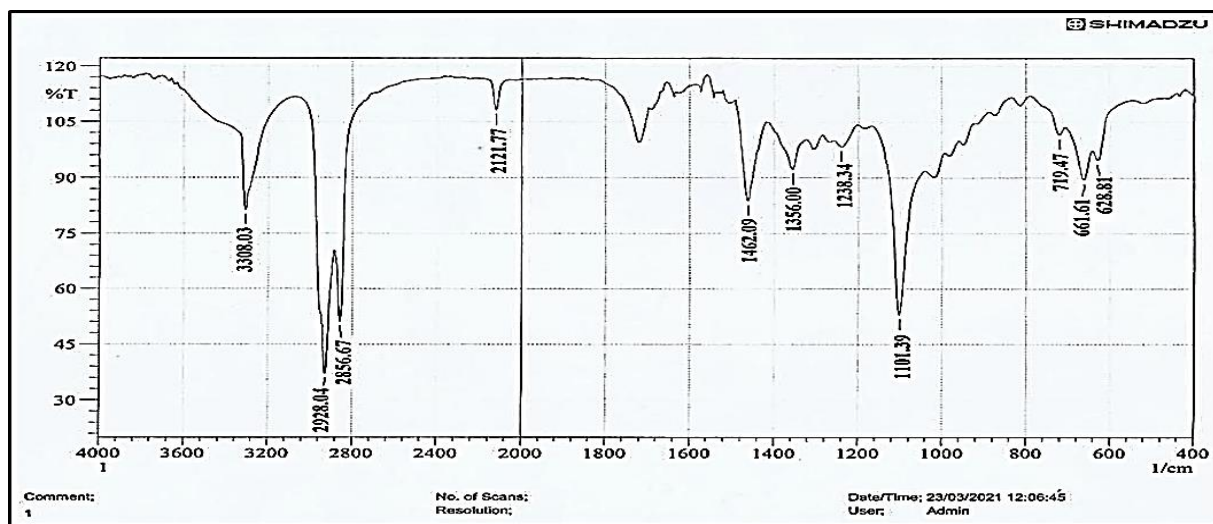


Figure 2. The spectrum of FT-IR of [BPMPD] compound.

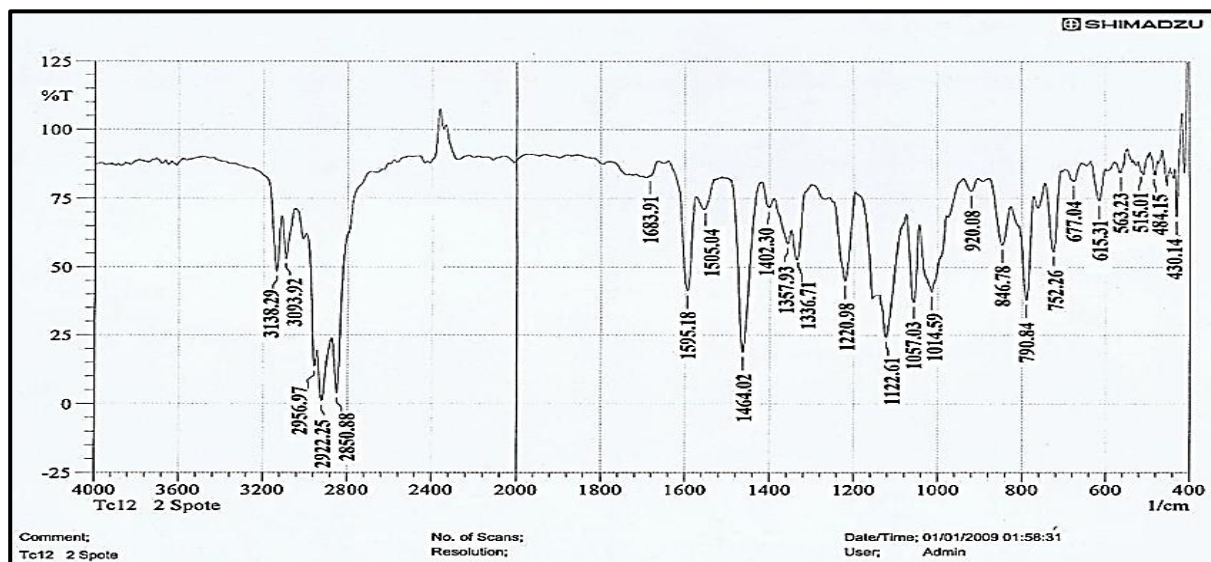


Figure 3. The spectrum of FT-IR of ligand [DTMML].

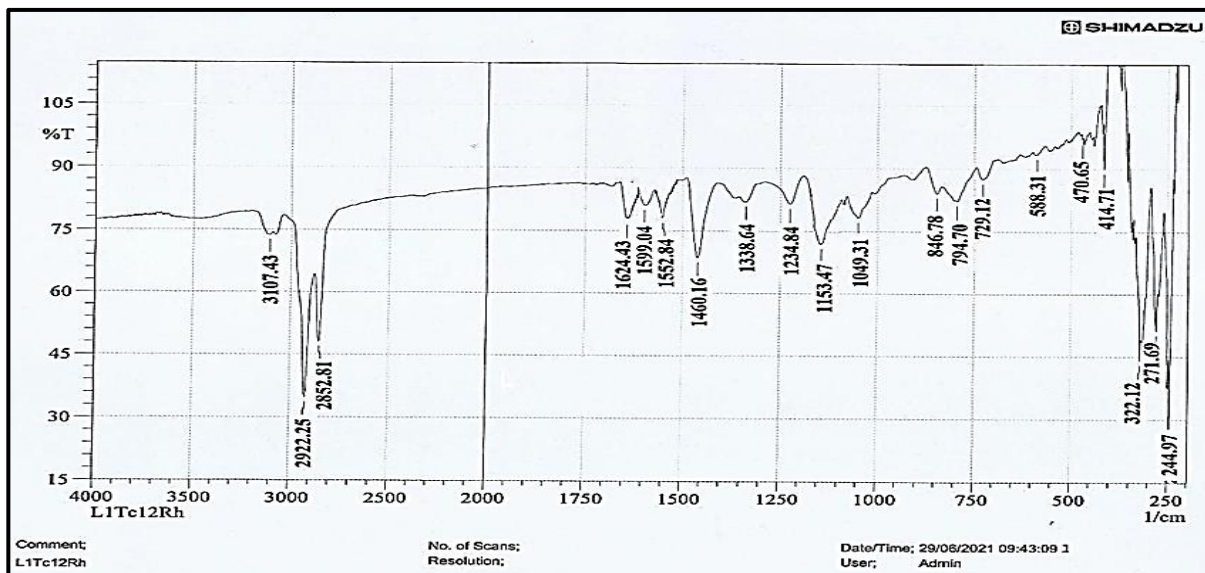


Figure 4. The spectrum of FT-IR of prepared complex of Rh(III).

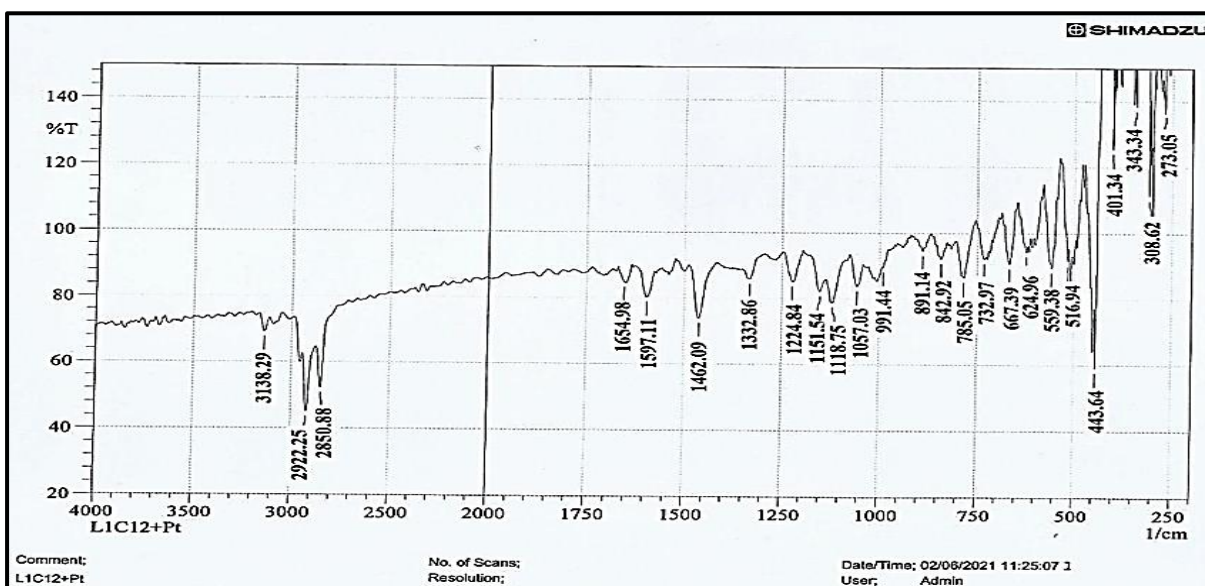


Figure 5. The spectrum of FT-IR of prepared complex Pt(IV).

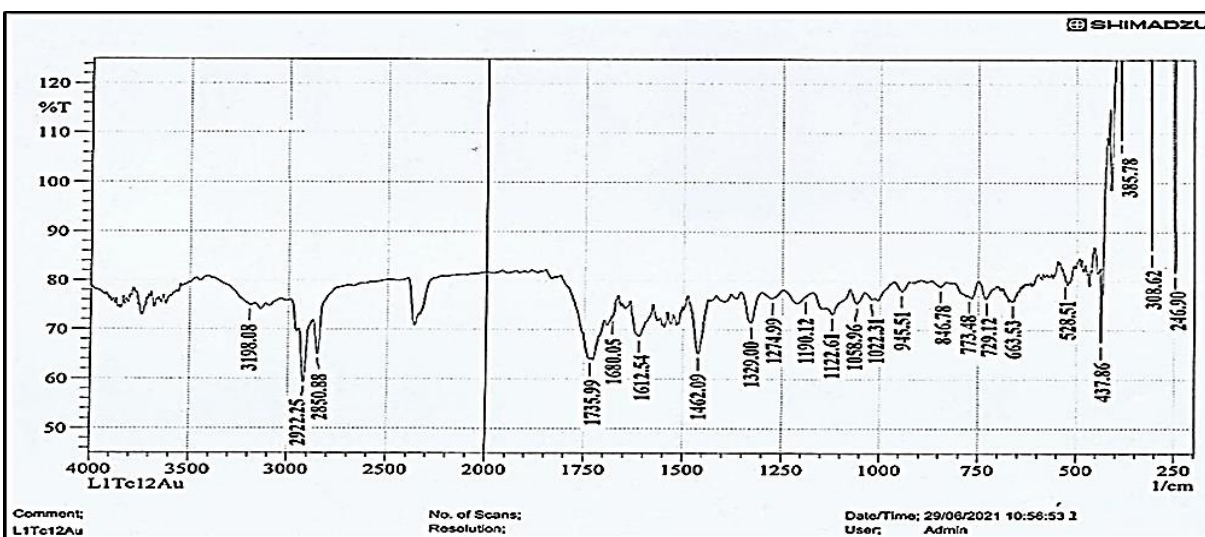


Figure 6. The spectrum of FT-IR of prepared complex of Au(III)

Table 2. Selected bands of the synthesized compounds' FT-IR spectra in  $\text{cm}^{-1}$ 

Compound	$\nu(\text{N}=\text{N})_{\text{triazole}}$	$\nu(\text{C}=\text{N})_{\text{pyridine}}$	$\nu(\text{C}-\text{N})_{\text{triazole}}$	$\nu(\text{C}-\text{O}-\text{C})_{\text{ether}}$	$\nu(\text{M}-\text{N})_{\text{pyridine}}$	$\nu(\text{M}-\text{O})$	$\nu(\text{M}-\text{N})_{\text{triazole}}$	$\nu(\text{M}-\text{Cl})$
L	1595.18	1505.04	1220.98	1122.61	-	-	-	-
L-Rh	1599.04	1552.84	1234.84	1153.47	271.69	414.71	588.31	322.12
L-Pt	1597.11	1553.99	1234.84	1150.75	273.34	443.64	516.94	308.62
L-Au	1680.05	1512.54	1274.99	1152.61	-	437.86	528.51	-

### Electronic spectra, Magnetic susceptibility and Conductivity measurements:

Additional structural tools were used to confirm the geometry of the produced complexes, from the data of electronic spectra, magnetic moment, and electrical measurements for their solution in DMSO. The complexes' uv-vis spectra were obtained in the region (190-1100) nm.

#### A-Spectra of the [DTMML]:

Figure.7, shows the electronic spectra of free ligand exhibited three bands at  $45662 \text{ cm}^{-1}$  which refer to the inter-correlation on the Pi system as ( $\pi \rightarrow \pi^*$ ) transition and at  $41841 \text{ cm}^{-1}$  that refer to ( $\pi \rightarrow \pi^*$ ) transition. The ( $n \rightarrow \pi^*$ ) electronic transition position on hetero atom of organic ligand (O and N) was attributed to the 3<sup>rd</sup> transition that appeared in  $37735 \text{ cm}^{-1}$ <sup>19</sup>. As shown in Table. 3.

#### B- Rhodium (III) complex:

Figure. 8 shows the electronic spectra of Rh(III) complex, displayed two absorption bands in the area  $31746$  and  $35714 \text{ cm}^{-1}$  which assigned to the  $^1\text{A}_{1g} \rightarrow ^1\text{T}_{2g}$  and  $^1\text{A}_{1g} \rightarrow ^1\text{T}_{1g}$  transition respectively. Another band appeared at  $11025 \text{ cm}^{-1}$  refer to spin prohibited transitions are a type of transition that can't happen  $^1\text{A}_{1g} \rightarrow ^3\text{T}_{1g}$ ,  $^3\text{T}_{2g}$ <sup>20</sup>. Magnetic moment measured (0.00 B.M.) of the solid state complex this align with the diamagnetic properties on octahedral stereochemistry of  $t_{2g}^6 e_g^0$  configuration<sup>21</sup>. As shown in scheme. 2. The conductance behavior of this complex indicates to an electrolyte. The calculation of conductivity for this complex in DMSO solvent at room temperature is a proof that it is ionic Table. 3.

#### C- Platinum(IV) complex:

Figure. 9 shows the electronic spectrum of a produced yellowish-orange complex of platinum (IV) ion, which showed two absorption bands at ( $27027$  and  $36363$ )  $\text{cm}^{-1}$  belonged to the transitions  $^1\text{A}_{1g} \rightarrow ^1\text{T}_{2g}$  and  $^1\text{A}_{1g} \rightarrow ^1\text{T}_{1g}$  respectively. The spin prohibited transitions can be attributed to the band that appeared in  $9990 \text{ cm}^{-1}$   $^1\text{A}_{1g} \rightarrow ^3\text{T}_{1g}$ ,  $^3\text{T}_{2g}$ <sup>22</sup>. These indicated an octahedral geometry as it came in agreement with reports. Magnetic moment of the solid complex was found to be (Zero B.M.). This result referred to spin pair octahedral stereochemistry referring to  $t_{2g}^6 e_g^0$  configuration<sup>23</sup>. The conductance behavior indicates an electrolyte of this complex. In addition, the analysis of data and spectroscopy techniques, and these result, proved that the octahedral geometry was suggested for this complex. As shown in scheme. 2, and Table. 3.

#### D- Gold (III) complex:

Figure.10 shows regarding the spectrum of complex of gold (III), showed two main bands at  $23923$ ,  $35842 \text{ cm}^{-1}$  which attributed to  $^1\text{A}_{1g} \rightarrow ^1\text{B}_{1g}$  &  $^1\text{A}_{1g} \rightarrow ^1\text{E}_g$  respectively and the other peak band appeared at  $44052 \text{ cm}^{-1}$  is considered as charge transfer transition around square planar geometry<sup>24</sup> and the magnetic moment which appeared diamagnetic with zero B.M. The conductivity measurement for this complex in DMSO solvent at room temperature shows ionic behavior. So from the analysis data and spectroscopy techniques for this complex, a square planar structure can be suggested. As shown in scheme. 2 and Table. 3.

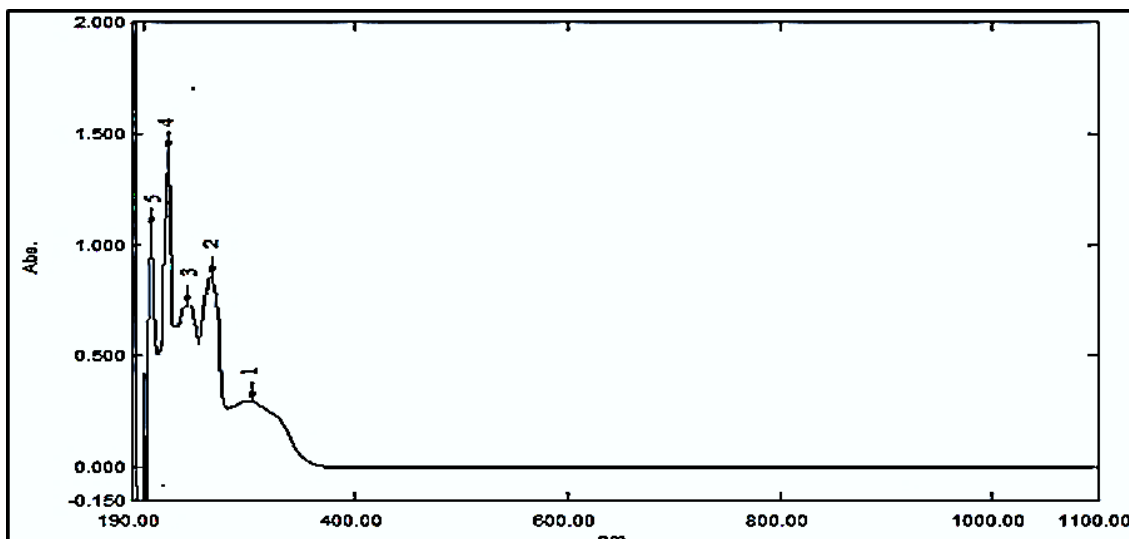


Figure 7. The electronic spectrum of the ligand [DTMML].

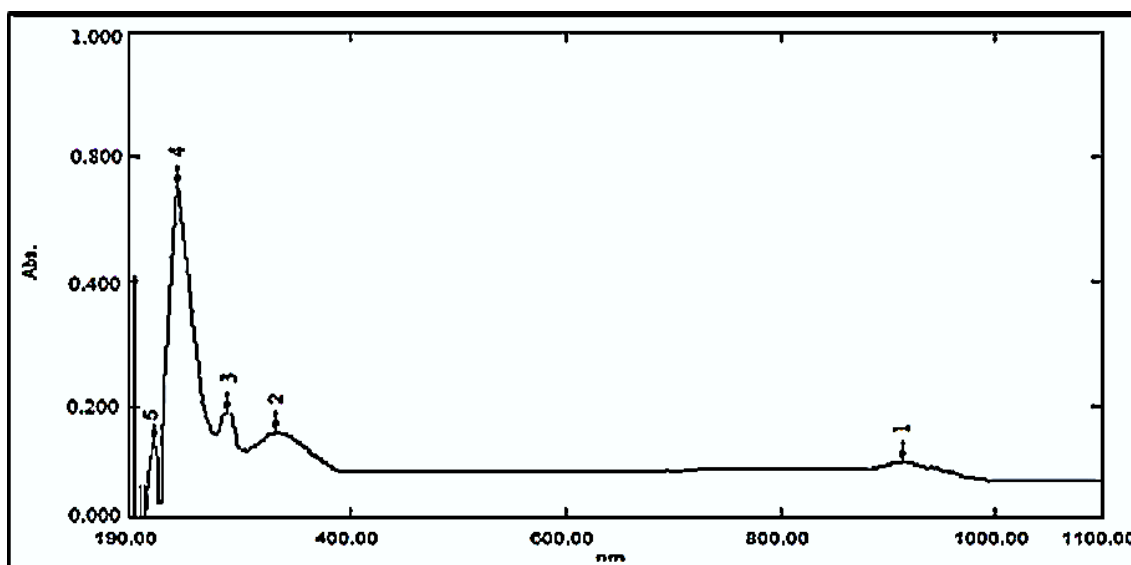


Figure 8. The electronic spectrum L-Rh(III) complex.

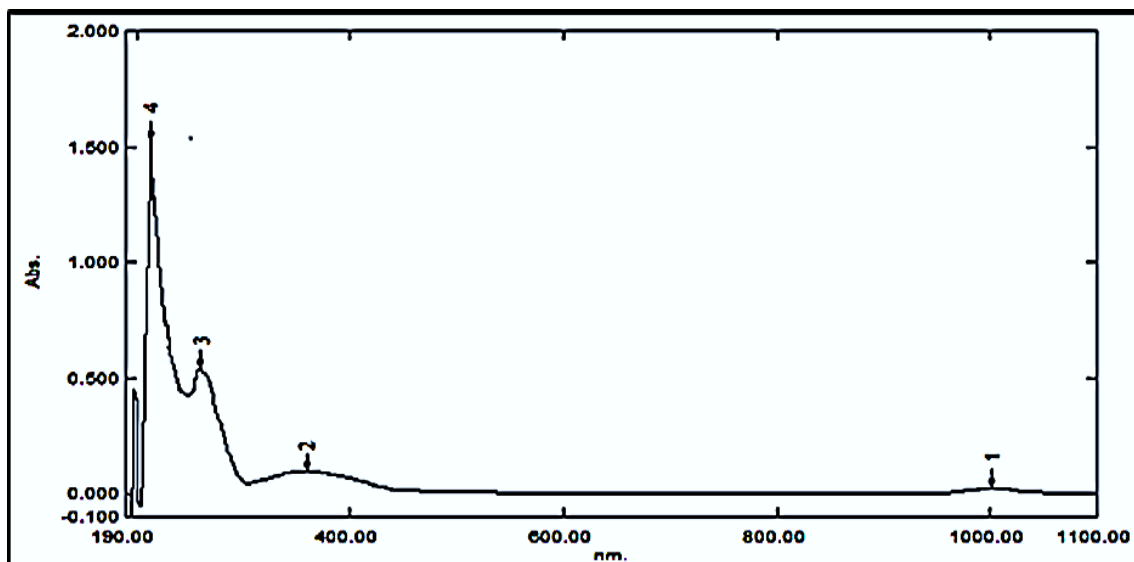


Figure 9. The electronic spectrum L- Pt(IV) complex.

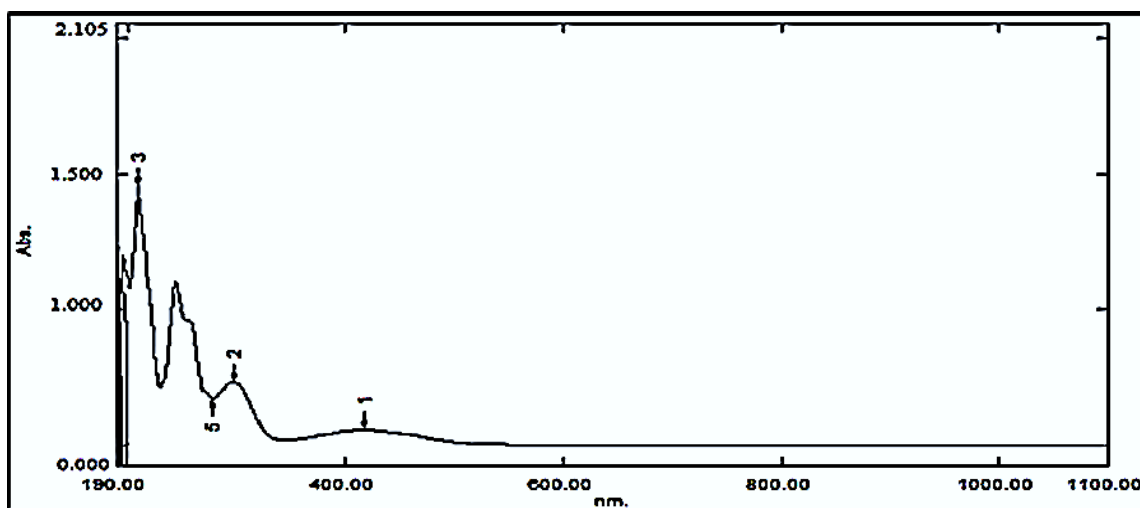
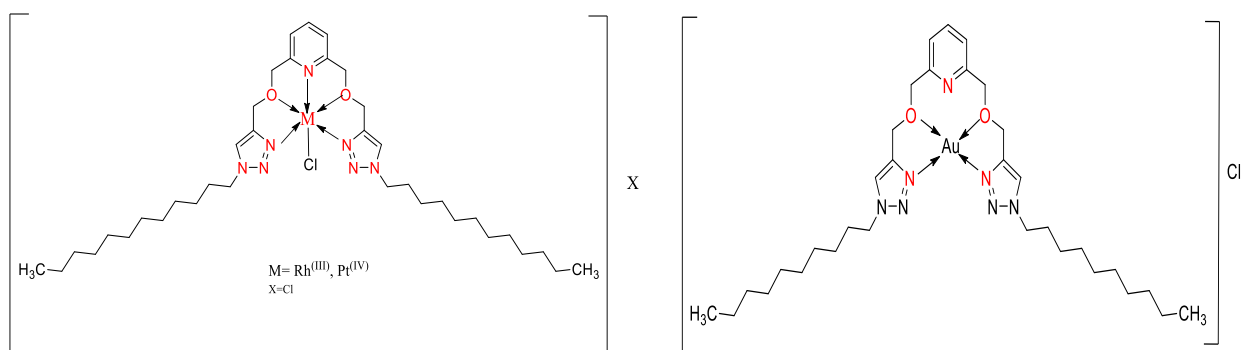


Figure 10. The electronic spectrum L-Au(III) complex.



Scheme 2. Proposed geometry of synthesized complexes.

Table 3. In a DMSO solvent, complex structural insights, electronic spectroscopy data, conductivity tests, and magnetic moments.

Compound s.	Absorbance $\text{cm}^{-1}$	Assignments	$\mu_{\text{eff}}$ B.M	$\mu\text{s. cm}^{-1}$	Suggested geometry
[DTMML]	37736 41841 45662	$n \rightarrow \pi^*$ $\pi \rightarrow \pi^*$	-	-	-
L-Rh	11025 31746 35714	$^1A_{1g} \rightarrow ^3T_{1g}, ^3T_{2g}$ $^1A_{1g} \rightarrow ^1T_{2g}$ $^1A_{1g} \rightarrow ^1T_{1g}$	0.00	72.7	Octahedral
L-Pt	9990 27027 36363	$^1A_{1g} \rightarrow ^3T_{1g}, ^3T_{2g}$ $^1A_{1g} \rightarrow ^1T_{2g}$ $^1A_{1g} \rightarrow ^1T_{1g}$	0.00	300.1	Octahedral
L-Au	23923 35842 44052	$^1A_{1g} \rightarrow ^1B_{1g}$ $^1A_{1g} \rightarrow ^1E_g$ $\text{Au} \rightarrow \text{LCT}$	0.00	280.1	Square planer

#### $^1\text{H-NMR}$ spectrum of the ligand and its complexes:

This ligand's  $^1\text{H-NMR}$  spectrum was displayed in Fig.11, where the DMSO- $d_6$  solvent was used to record the data. The spectrum showed peaks at  $\delta$  (1.83-0.83) ppm (d, 2H,  $\text{H}_2$ - $\text{H}_9$  and  $\text{H}_{25}$ - $\text{H}_{32}$ ) which, as a result of the protons of ( $\text{CH}_2$ ) numerous peaks and aliphatic series groups appeared in the range  $\delta$  (8.16-

7.33) ppm (t, H,  $\text{H}_{16}$ - $\text{H}_{18}$ ) and (s,  $\text{H}_{11}$ ,  $\text{H}_{23}$ ) that back to the groups of (-CH) in pyridine<sup>25</sup>, in addition to the protons in the triazole ring, as well as a peak appeared in the range  $\delta$  (4.64-4.58) ppm (d, 2H,  $\text{H}_{10}$ ,  $\text{H}_{24}$ ,  $\text{H}_{14}$  and  $\text{H}_{20}$ )  $\text{CH}_2$ . The aliphatic chain's initial group is connected with the ring of triazole and methylene linked in ring of pyridine. Furthermore, signal is shown as peaks on the chart  $\delta$

(4.35-4.32) ppm (s, 2H, H<sub>13</sub> and H<sub>21</sub>)<sup>26</sup>. The comparison of <sup>1</sup>H-NMR Pd(II) complex spectra created with the proton's ligand spectrum location approximately confirming the coordination, shifting

of the position of proton of the ligand is very small when compared with these metal complexes. At (2.51) ppm, the DMSO shows a singlet peak, all shown in Fig. 12.

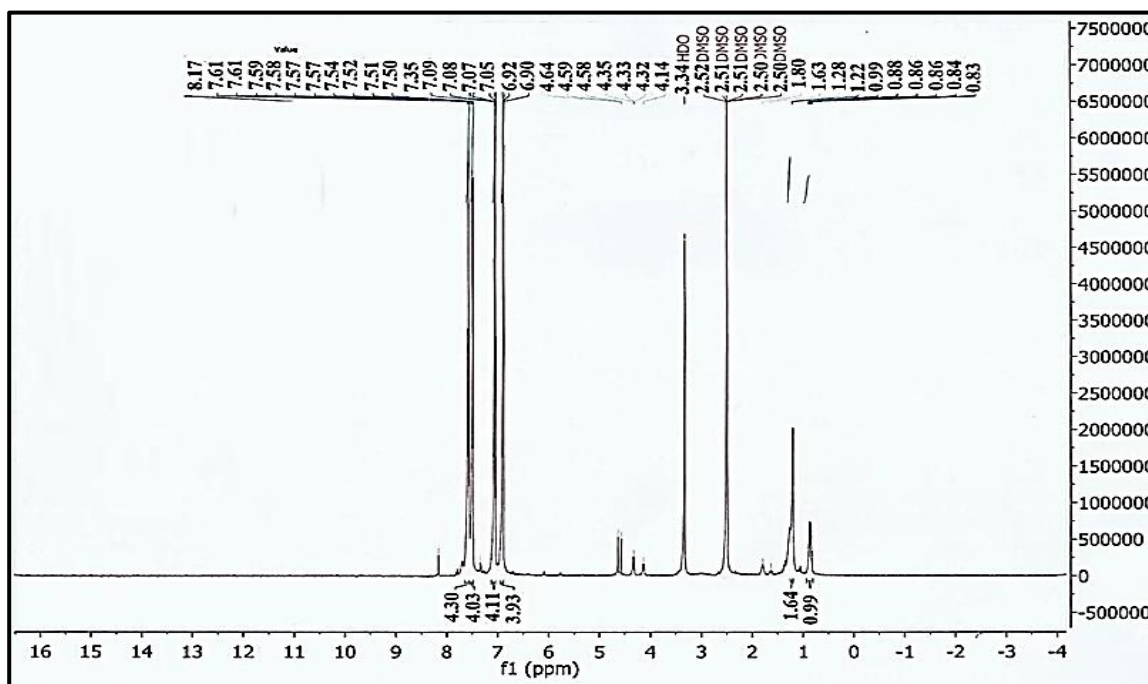


Figure 11. Spectrum of <sup>1</sup>H-NMR of the [DTMML].

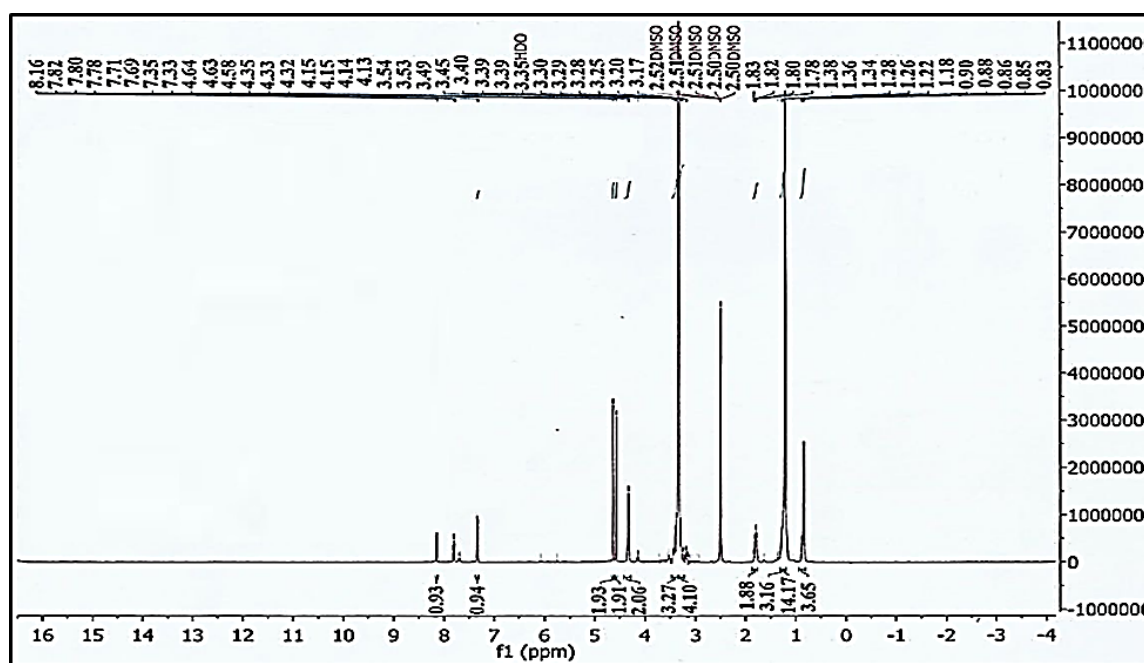


Figure 12. Spectrum of <sup>1</sup>H-NMR of the [L-Pd(II)]

#### Mass spectrum for ligand:

The mass spectrum of (L) shown in Fig. 13, was observed by the peak of molecular ion at  $m/z = 637$  which confirmed the molecular weight  $m/z$  value of

$637 \text{ g mol}^{-1}$  that compatible with the experimental ligand formula ( $\text{C}_{37}\text{H}_{63}\text{N}_7\text{O}_2$ )<sup>27</sup>. Scheme. 3 involving fragments ions in mass spectra.

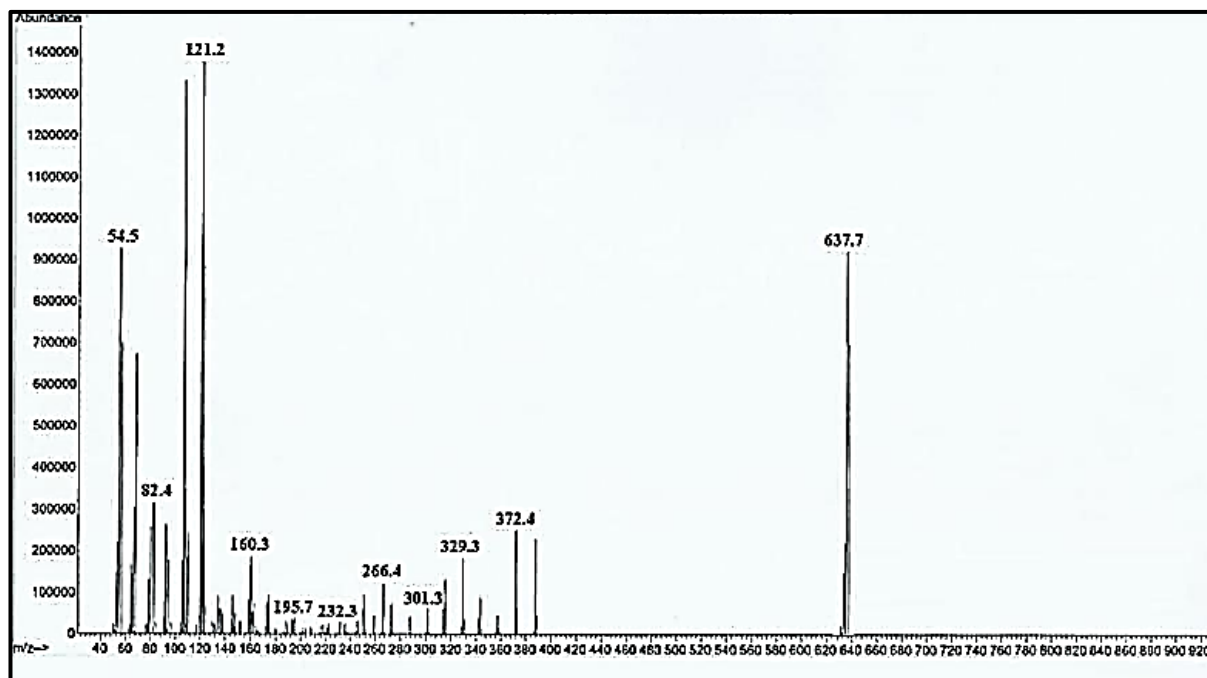
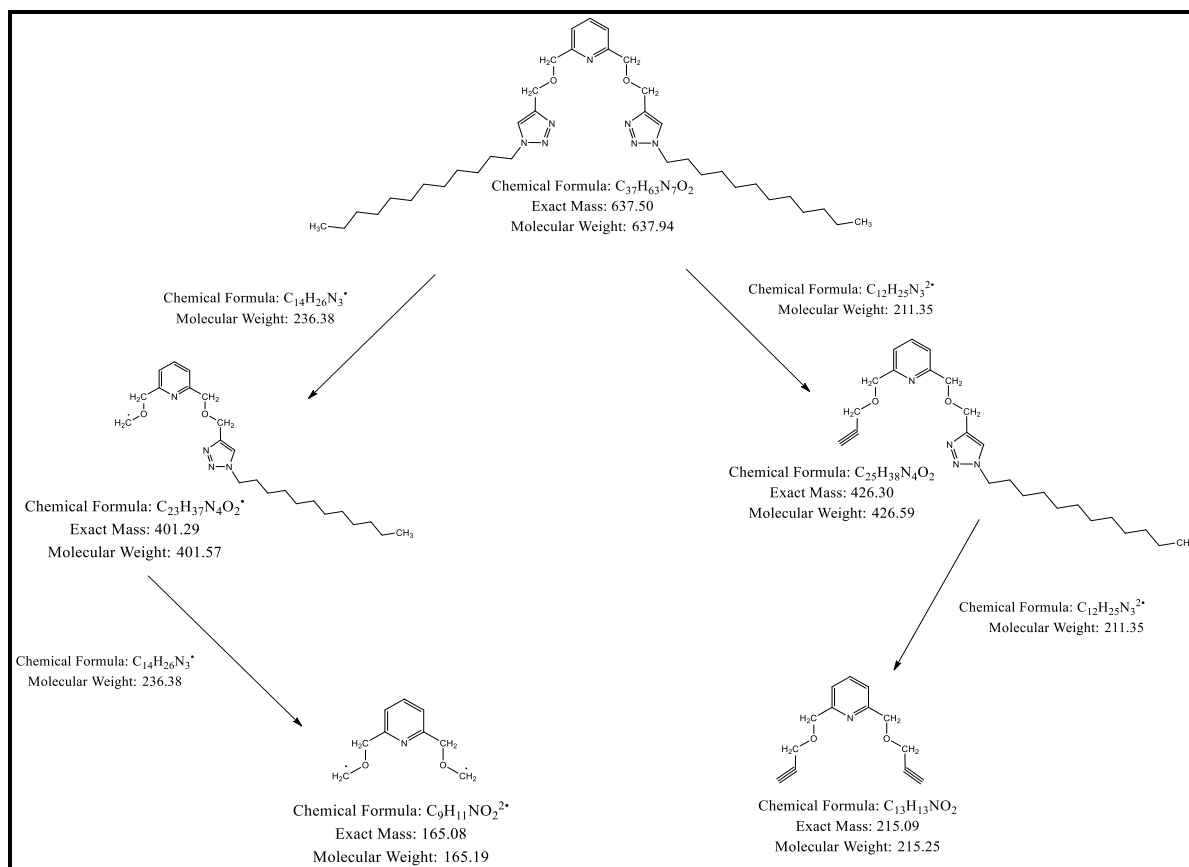


Figure 13. Mass spectrum of [DTMML].



Scheme 3. Fragments ions in mass spectra for [DTMML].

### Cytotoxic assay:

Breast cancer is the popular type of tumors for women in the worldwide, which represents approximately twenty-five percent of all female malignant tumors which has extend widely in most countries, even developed countries<sup>28</sup>. Furthermore, despite the fact that many additional medications

have been launched to the market, the response to therapy remains low. As a result, there is a pressing need to produce more effective anticancer medications<sup>29</sup>. Most research groups are focus on developing a practical anticancer medicine that can be utilized effectively to treat human cancers. This study gives? indication that the synthetic ligand and

its complexes have efficacious action verses breast cancer MDA-MB-231 cell lines (in vitro). The data are summarized in Table 4, Least Significant Difference (LSD Value) is recorded in this table also.

MTT assay was applied to assess cytotoxicity and viability of the MDA-MB-231 cell lines after 24 hours of treating by different concentrations (12.5; 25; 50; 100; 200 and 400)  $\mu\text{g/ml}$  of newly prepared compounds (Table. 4 and Fig. 14). MTT assay results showed a high inhibition rates for free ligands and their metal complexes as comparison with negative control cells which left without treatment. All metal complexes showed high toxicity relative to ligand and recorded high inhibition rate i.e. (85, 85 & 84 %) especially at high concentrations 400 $\mu\text{g/ml}$  for each of L-Rh, L-Pt and L-Au sequentially and the inhibition rates began to reduce gradually from high to low concentrations. Pharmacological effects of these complexes can be returned to variety circumstances, such as, synthetic derivatives in a similar manner to natural material follow apoptosis and autophagic pathways to inhibit the growth and activity of breast cancer cells. Other than that

inhibition of cell proliferation, induction of cell-cycle arrest may occur<sup>30</sup>. As well as presence of 1,2,3-Triazole could be readily interact with diverse enzymes. Our current work highlights in 1,2,3-triazole-containing compounds with anti-breast cancer potential, and their structure-activity relationship (SAR) together with of action to pave the way for the further rational development of novel anti-breast cancer mechanisms candidates. On the other hand, Pyridines are potential inhibitors and some pyridine-based agents, have already been applied in clinical practice or under clinical trials for the treatment of cancers<sup>31</sup>. Thus, gathering of 1,2,3-triazole with pyridine may give chances to develop new anticancer agents. An antiproliferative SAR of 1,2,3-triazole-containing pyridine derivatives against cell lines indicates that these groups are favorable for the<sup>32</sup>. The most active compounds exhibit higher activity than the others concentrations reveal that these compounds in high concentration could inhibit the microtubule assembly, arrest the cell cycle at the G2/M phase, and induce cell death by apoptosis<sup>31</sup>.

**Table 4. Shows the percentage inhibition rate on MDA cells lines**

Comp.	Conc. ( $\mu\text{g/mL}$ )						LSD value
	C 400	C200	C100	C50	C25	C12.5	
L <sub>3</sub>	60%	54%	34%	27%	19%	15%	7.95 **
L <sub>3</sub> Rh	85%	59%	45%	35%	27%	22%	9.29 **
L <sub>3</sub> Pt	85%	59%	47%	42%	42%	41%	8.63 **
L <sub>3</sub> Au	84%	66%	55%	52%	51%	31%	8.79 **
LSD value	7.81 **	6.77 **	6.07 **	8.46 **	7.17 **	7.53 **	---

The means of distinct big characters in the same column and little letters in the same row varies dramatically. \*\* (P $\leq$ 0.01).

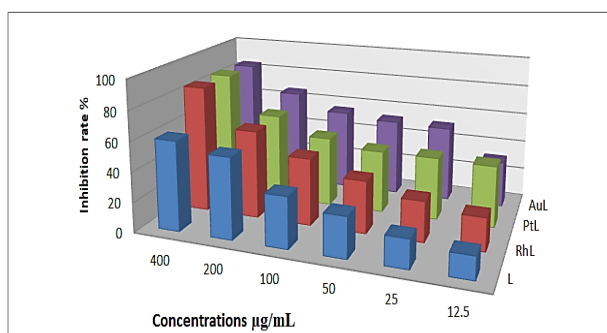


**Figure 14. The diagram of inhibition rate as a percentage on MDA cell line after 24 hours of exposure to prepared compounds.**

### Conclusion:

According to the findings, new derivative of triazole [DTMML] and spectroscopic tests, analysis of elements (AA & CHNS), magnetic dipole moment, and complexes conductivity at room temperature were used to validate the structure of its complexes. In the solid state, we propose that Rh(III) and Pt(IV) complexes have six coordination numbers with octahedral geometries, whereas the Au(III) complex has four coordination numbers with square planer shape. The anticancer MDA cell line was used to test these substances, and it was discovered that the higher the concentration, the more efficient they are against cancer cells. For these complexes, the

synergetic effect has a higher biological activity than the free ligand.

#### Authors' declaration:

- Conflicts of Interest: None.
- We hereby confirm that all the Figures and Tables in the manuscript are mine ours. Besides, the Figures and images, which are not mine ours, have been given the permission for re-publication attached with the manuscript.
- Authors sign on ethical consideration's approval
- Ethical Clearance: The project was approved by the local ethical committee in University of Kerbala.

#### Authors' contributions statement:

J. H. A., role Conception, design, acquisition of data signature. M. F. A. role analysis, interpretation, drafting the MS, revision and proofreading signature.

#### References:

1. El Azab IH, El-Sheshtawy HS, Bakr RB, AA Elkanzi N. New 1, 2, 3-triazole-containing hybrids as antitumor candidates: design, click reaction synthesis, DFT calculations, and molecular docking study. *Molecules*. 2021 Jan; 26(3): 708.
2. Xu Z, Cheng G, Yang H, Zhang J, Shreeve JN. Synthesis and Characterization of 4-(1, 2, 4-Triazole-5-yl) furazan Derivatives as High Performance Insensitive Energetic Materials. *Chem Eur J*. 2018 Jul 20; 24(41): 10488-97.
3. El Azab IH, Elkanzi NA. An efficient synthetic approach towards Benzo [b] pyrano [2, 3-e][1, 4] diazepines, and their cytotoxic activity. *Molecules*. 2020 Jan; 25(9): 2051.
4. Rani P, Lal K, Shrivastava R, Ghule VD. Synthesis and characterization of 1, 2, 3-triazoles-linked urea hybrid sensor for selective sensing of fluoride ion. *J Mol Struct.* 2020 Mar 5; 1203: 127437.
5. Farrer NJ, Griffith DM. Exploiting azide-alkyne click chemistry in the synthesis, tracking and targeting of platinum anticancer complexes. *Curr Opin Chem Biol*. 2020 Apr 1; 55: 59-68.
6. El Azab IH, Elkanzi NA, Gobouri AA. Design and Synthesis of Some New Quinoxaline Based Heterocycles. *J Heterocycl Chem*. 2018 Jan; 55(1): 65-76.
7. Riddell IA, Lippard SJ. Cisplatin and oxaliplatin: our current understanding of their actions. *Met Ions Life Sci*. 2018 Feb 5; 18: 1-42.
8. Kitteringham E, Zhou Z, Twamley B, Griffith DM. Au (III) and Pt (II) complexes of a novel and versatile 1, 4-disubstituted 1, 2, 3-triazole-based ligand possessing diverse secondary and tertiary coordinating groups. *Inorg Chem*. 2018 Sep 7; 57(19): 12282-90.
9. Jihan HA, Mahasin FA. Synthesis, Characterization and Antimicrobial Activity of Cu(II), Pt(IV) and Au(III) Complexes with 2,6-bis(((1-decyl-1H-1,2,3-triazole-4-yl)methoxy)methyl)pyridine. *Chem Methodol*. 2022; 6(3): 184-196.
10. Al-Radadi NS, Zayed EM, Mohamed GG, Abd El Salam HA. Synthesis, Spectroscopic Characterization, Molecular Docking, and Evaluation of Antibacterial Potential of Transition Metal Complexes Obtained Using Triazole Chelating Ligand. *Hindawi*. 2020 February 24; 1-12.
11. Ibrahim AA, Kareem MM, Al-Noor TH, Al-Muhimeed T, AlObaid AA, Albukhaty S, et al. Pt (II)-Thiocarbohydrazone complex as cytotoxic agent and apoptosis inducer in Caov-3 and HT-29 cells through the P53 and Caspase-8 pathways. *Pharmaceuticals*. 2021 Jun; 14(6): 509.
12. Yao K, Bertran A, Howarth A, Goicoechea JM, Hare SM, Rees NH, et al. A visible-light photoactivatable di-nuclear Pt IV triazolato azido complex. *Chem Comm*. 2019; 55(75): 11287-90.
13. Savaş B, Öztürk T, Meyvacı E, Hazer B. Synthesis and characterization of comb-type graft copolymers by redox polymerization and "click" chemistry method. *SN Appl Sci*. 2020 Feb; 2(2): 1-8.
14. Englinger B, Pirker C, Heffeter P, Terenzi A, Kowol CR, Keppler BK, et al. Metal drugs and the anticancer immune response. *Chem Rev*. 2018 Nov 29; 119(2): 1519-624.
15. Samarasimhareddy M, Shamir M, Shalev DE, Hurevich M, Friedler A. A rapid and efficient building block approach for click cyclization of peptoids. *Front Chem*. 2020 May 19; 8: 405-420.
16. Saeed AA, Jassim AH, Ahmed MF. Determination of the Ratios of Ligands to Metal Ion of some Metal Complexes of Triazoles by Using Electronic Spectra in Organic Solvents. *Baghdad Sci J*. 2004; 1(1): 110-115.
17. Peng K, Mawamba V, Schulz E, Löhr M, Hagemann C, Schatzschneider U. iClick reactions of square-planar palladium (II) and platinum (II) azido complexes with electron-poor alkynes: metal-dependent preference for N1 vs N2 triazolite coordination and kinetic studies with <sup>1</sup>H and <sup>19</sup>F NMR spectroscopy. *Inorg Chem*. 2019 Aug 8; 58(17): 11508-21.
18. El Malah T, Nour HF, Satti AA, Hemdan BA, El-Sayed WA. Design, synthesis, and antimicrobial activities of 1, 2, 3-triazole glycoside clickamers. *Molecules*. 2020 Jan; 25(4): 790.
19. Mohamad HA, AL-Kattan WT, AL-Daly ZM. Synthesis, Characterization and Cytotoxicity of Ni (II), Pd (II), Pt (II) Complexes with 6-Methoxy-2, 3, 4, 5-tetrahydropyridine (MTP). *Chemistry*. 2020 July 20; 36(5): 903-907.
20. Burke HM, Gallagher JF, Indelli MT, Vos JG. The synthesis and characterisation of Rh (III) complexes with pyridyl triazole ligands. *Inorganica Chim Acta*. 2004 Jul 20; 357(10): 2989-3000.
21. Burke HM, Gallagher JF, Indelli MT, Vos JG. The synthesis and characterisation of Rh (III) complexes with pyridyl triazole ligands. *Inorganica Chim Acta*. 2004 Jul 20; 357(10): 2989-3000.
22. Mohamad HA, Al-Kattan WT, Al-Daly ZM. Synthesis, Characterization and Cytotoxicity of Ni (II),

- Pd (II), Pt (II) Complexes with 6-Methoxy-2, 3, 4, 5-tetrahydropyridine (MTP). Chemistry. 2020 July 20; 36(5): 903-907.
23. Al-Hamdani AAS, Hamoodah RG. Transition metal complexes with tridentate ligand: preparation, spectroscopic characterization, thermal analysis and structural studies. Baghdad Sci J. 2016; 13(4): 770-781.
24. Shayma AS, Mohammed HA, Al-Hamdani AAS. Preparation, Physico-Chemical and Spectroscopic Investigation of Thiacetazone and Quinalizarin Complexes with Mn(II), Fe(II), Co(II), Ni(II), Cu(II), Zn(II), Cd(II) and Pb(II). Austr J Basic Appl.Sci. 2010;4(10): 5178-5183.
25. Zhang Y, Chu CW, Ma W, Takahara A. Functionalization of Metal Surface via Thiol-Ene Click Chemistry: Synthesis, Adsorption Behavior, and Postfunctionalization of a Catechol-and Allyl-Containing Copolymer. ACS Omega. 2020 Mar 26; 5(13): 7488-96.
26. Kollaschinski M, Sobotta J, Schalk A, Frischmuth T, Graf B, Serdjukow S. Efficient DNA Click Reaction Replaces Enzymatic Ligation. Bioconjug Chem. 2019 Dec 24;31(3):507-12.
27. Stefanetti G, Allan M, Usera A, Micoli F. Click chemistry compared to thiol chemistry for the synthesis of site-selective glycoconjugate vaccines using CRM197 as carrier protein. Glycoconj J. 2020 Oct; 37(5): 611-22.
28. Sharmin S, Rahaman M, Martorell M, Sastre-Serra J, Sharifi-Rad J, Butnariu M, et al. Cytotoxicity of synthetic derivatives against breast cancer and multi-drug resistant breast cancer cell lines: a literature-based perspective study. Cancer Cell Int. 2021 Dec; 21(1): 1-9.
29. AlSaady TA, Madlum KN, Obied HN. Effect of antioxidants on cisplatin-induced cytotoxicity and oxidative stress in colon cancer cells. Eur Asian J Biosci. 2020 Aug 1; 14(2).
30. Rocha AM, Sousa FS, Borba VM, Munchen TS, Leal JG, Rodrigues OE, et al. Evaluation of the effect of synthetic compounds derived from azidothymidine on MDA-MB-231 type breast cancer cells. Bioorganic Med Chem Lett. 2020 Sep 1; 30(17): 127365.
31. Liang T, Sun X, Li W, Hou G, Gao F. 1, 2, 3-Triazole-Containing Compounds as Anti-Lung Cancer Agents: Current Developments, Mechanisms of Action, and Structure-Activity Relationship. Front Pharmacol. 2021; 12.
32. Prasad B, Nayak VL, Srikanth PS, Baig MF, Reddy NS, Babu KS, et al. Synthesis and biological evaluation of 1-benzyl-N-(2-(phenylamino) pyridin-3-yl)-1H-1, 2, 3-triazole-4-carboxamides as antimitotic agents. Bioorganic Chem. 2019 Mar 1; 83: 535-48.

## معقدات المعادن الثقيلة من مشتق 3,2,1- ترايزول : تحضير، تشخيص و تقييم السمية الخلوية ضد خطوط خلايا سرطان الثدي (231-MDA-MB)

محاسن فيصل الياس<sup>2</sup>

جهان حميد عبد الامير<sup>1</sup>

<sup>1</sup> كلية التربية والعلوم الصرفة، جامعة كربلاء، العراق.

<sup>2</sup> قسم الكيمياء، كلية العلوم للبنات، جامعة بغداد، بغداد، العراق.

### الخلاصة:

تم تحضير ليكاندات مخلبية جديدة مشتقة من الترايزول ومعقداته اللاعضوية مع الايونات الفلزية لكل من الروديوم و البلاتين و الذهب. حُضر الليكاند من تفاعل bis((prop-2-yn-1-yloxy) methyl) pyridine-2,6 مع azidododecane-1 من خلال تفاعل الاضافة الحلقية ثنائية القطب بوجود ايون النحاس الاحادي كعامل مساعد. استخدمت تقنيات طيفية و فحوصات فيزيائية مختلفة لتشخيص الهيكل البنائي للمركبات المحضرة في الحالة الصلبة و من هذه التقنيات ( طيف الرنين النووي المغناطيسي، طيف الاشعة فوق البنفسجية-الطيف المرئي، طيف الاشعة تحت الحمراء، تحليل العناصر و الفلزات، الحساسية المغناطيسية، قياسات التوصيلية الكهربائية في درجة حرارة الغرفة ) و تم التوصل الى ان الليكاند المحضر يسلك كليكاند خماسي السن في بعض المعقدات و كرباعي السن في معقدات اخرى من خلال ذرات النيتروجين و الاوكسجين المانحة (N<sub>3</sub>O<sub>2</sub>, N<sub>2</sub>O<sub>2</sub>) و ان الشكل الهندسي لمعقدات الروديوم و البلاتين هو ثماني السطوح بينما يكون مربع مستوي لمعقد الذهب. تم تقييم فعالية الليكاند المحضر ومعقداته كمضادات للسرطان داخل المختبر ضد MDA cell lines ومن خلال نتائج التقييم يمكن الاستنتاج بان المركبات المحضرة ترتقي لان تستخدم كمضادات سرطانية في المستقبل خاصة عند استخدام التراكيز العالية منها.

**الكلمات المفتاحية:** المقايسة الحيوية، معقدات ليكاند مخلبي، خط الخلية MDA، مجموعة الميثوكسي، السمية الخلوية، ترايزول.